Massive gas injection from the high field side of ASDEX Upgrade

G. Pautasso, K. Mank, A. Mlynek, M. Beck, W. Weisbart, M. Bernert,
O. Gruber, A. Herrmann, M. Sertoli and the ASDEX Upgrade Team
Max-Planck-Institut für Plasmaphysik, EURATOM Association, D-85748 Garching, Germany
E-mail contact of main author: gabriella.pautasso@ipp.mpg.de

Introduction.

The critical electron density, n_c, required to assure the collisional suppression of runaway electrons in ITER disruptions is of the order of 4×10^{22} m^{-3} [1]. In experiments made in ASDEX Upgrade (AUG) in 2009 [2], an effective electron density equivalent to 24 % of $n_{c,\,AUG}$ was attained by injecting 3.3 bar·l of neon with a fast valve located on the low field side (LFS) at the midplane ($n_{c,\,AUG}$ is the actual value of n_c, calculated with the measured internal inductivity and current decay rate). At this large amount of injected impurities, the fuelling efficiency (F_{eff}) remained at the level of 20 % for plasmas with a modest thermal energy (E_{th} < 0.4 MJ). Nevertheless, a significant decrease of the F_{eff} with increasing plasma E_{th} was observed at large amounts of injected helium and neon atoms. This was interpreted as an **E**×**B** drift effect, which had been previously observed to prevent or favor deeper fuel penetration and higher F_{eff} of pellets when launched respectively from the low or high field side (HFS) of the torus. In order to verify this interpretation, a new valve was developed and mounted on the AUG HFS during the 2010 vessel opening. The preliminary experiments, presented in this contribution, show that the new HFS valve has a significantly higher F_{eff} than the LFS one.

The valve.

The HFS fast valve is located in sector 13, 50 cm above the mid-plane, 10 cm behind the limiting surface defined by the heat shield (fig. 1, left). The valve stem is kept in the closed-valve position by 3 pairs of piezo-actuators, which expand under an applied voltage of ~ 100 V. A disk-spring package moves back the stem and opens the valve, as soon as a trigger causes the discharge of the piezos. The new HFS valve has a gas reservoir volume (85 cm^3), opening time (1 ms), nozzle area (1.23 cm^2) and maximum reservoir pressure (50 bar) similar to the older LFS valve [2] (80 cm^3, 1 ms, 1.54 cm^2 and 50 bar respectively). Nevertheless, it was dimensioned anew, in order to make it fit between the HFS vessel wall and the heat shield, where there is less space than on the LFS. The number of piezo-actuator pairs, holding the stem of the valve in the closed position had to be reduced from 4 (LFS valve) to 3 and located on the same plane (fig. 1, center). The HFS valve was designed to release most of the gas

contained in the reservoir before the beginning of the current quench. The time delay between the trigger and the arrival of the gas at the plasma edge, as detected by the AXUV (Absolute eXtreme UltraViolet) diagnostic, is of the order of 1 ms. Assuming a movement of the stem linear in time (2.8 mm within 1 ms) and ideal flow, the pressure in the valve and the quantity of gas released in the vessel have been calculated and shown on the right side of fig. 1.

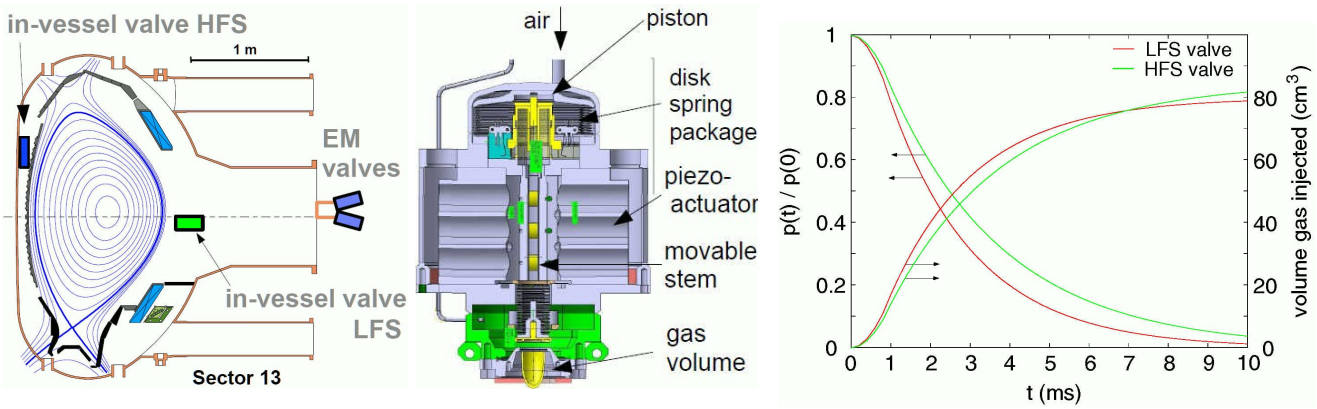

Figure 1. Left: location of the mitigation valves in AUG. Center: cross section of the HFS valve. Right: time evolution of the pressure, p(t), in the valve and integrated volumetric gas flow.

Experimental conditions.

The number of discharges, shut-down with the HFS valve, is presently limited to 5, because of a premature failure of the valve stem. The target plasmas had a toroidal current of 1 MA, $q_{95} = 4.7$ and different values of E_{th} (0.1-0.2 MJ and 0.4-0.6 MJ). Neon, with a starting reservoir pressure of 10 and 20 bar, was injected in 4 discharges and helium at 20 bar was used once. The concentration of neon in discharges following MGI (massive gas injection) shut-down was measured with the Bragg-spectrometer and found to be of the order of 10^{-4}.

Fuelling efficiency.

The CO_2-laser interferometer can provide measurements of the line integrated density along two vertical chords after MGI. In all cases of HFS MGI, the electron density is seen to rise to a level, which is roughly twice the one reached after LFS MGI. Fig. 2 shows the time traces of plasma parameters after a LFS and a HFS MGI shut-down with circa 0.8 bar·l of neon, and the larger density reached in the second case. Following [2], the F_{eff} is calculated as the ratio of the line integrated density measurements, averaged over the plasma during the current quench, and the total quantity of gas injected by the valve. F_{eff} is found to be in the range 35-55 % (compared to 20-30 % for LFS MGI), increasing with the plasma energy and decreasing with the quantity of injected neon, as shown on the left of fig. 3. Helium did not manifest a F_{eff} larger than neon, as in the LFS MGI; nevertheless the

number of helium MGIs is very limited to draw conclusions. It is worth noticing that the ratio between

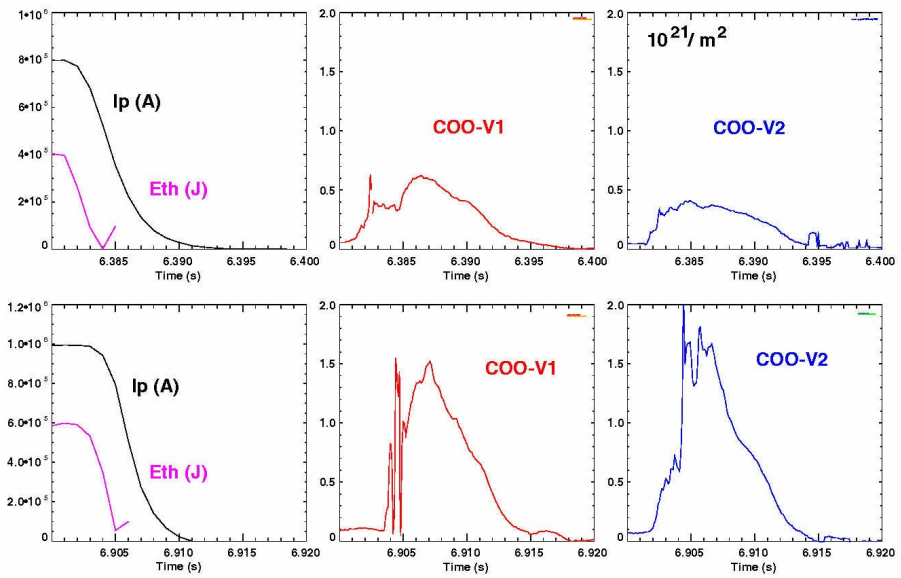

Figure 2. Time traces of plasma current (I_p), energy (E_{th}) and line integrated density along the V-1 and V-2 cord of the CO_2 inter-ferometer for a LFS MGI (above) and a HFS MGI (below) shut-down with 0.8 bar· l of neon.

the increase of the total number of electrons in the plasma and the actual number of atoms injected by the valve is larger than F_{eff} since, at the time of maximum n_e, 10-20 % of the gas is still in the valve. Although it is reasonable to attribute the larger HFS F_{eff} to the **E×B** drift, there is no direct experimental observation of it at the moment. The larger F_{eff} of pellets injected from the HFS were clearly accompanied by the observation of the acceleration of the pellet in plasma and a larger penetration depth of the pellet [3].

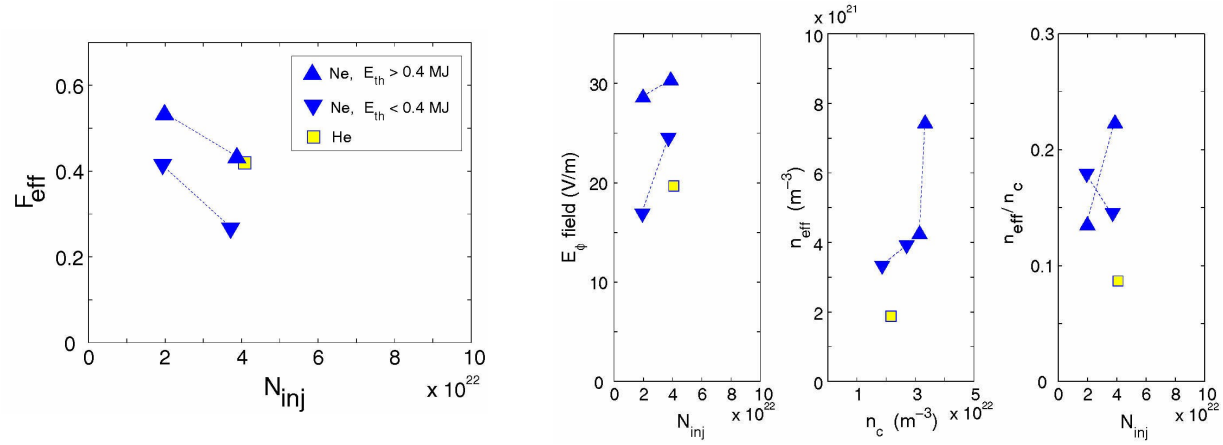

Figure 3. Left: dependence of the fuelling efficiency (F_{eff}) on the number of injected atoms, (N_{inj}) and the plasma thermal energy (E_{th}). Right: the toroidal electric field (E_ϕ) versus N_{inj}, the effective density (n_{eff}) versus the critical electron density (n_c) and n_{eff}/n_c versus N_{inj}.

After MGI, the AXUV radiation emission measurements show the penetration of the injected gas into the plasma during the cooling phase, that is between the arrival of the gas at the plasma edge and the thermal quench. Nevertheless this penetration does not appear faster and/or deeper in case of the HFS

compared to the LFS injection, but rather slower and shallower. Particularly in the cases of HFS neon injection in plasmas with $E_{th} > 0.4$ MJ, the cooling phase last twice longer than in the LFS, independently of E_{th}, and HFS cases with $E_{th} < 0.4$ MJ. After the thermal quench, impurities are redistributed over the whole plasma and the differences between LFS and HFS MGI disappear. Support from theoretical modelling is required to postulate the time and place of occurrence of the inward drift. An important role in the higher HFS F_{eff} should also be played by the wall, which is close to the plasma and reflects the neutral particles, not ionized in the plasma, back into it, increasing the probability of assimilation. On the contrary, the LFS valve is mounted on the side wall of a port and the injected atoms, which are once reflected by the plasma, can expand in a large volume and have a small probability of being ionized in the plasma.

The average toroidal electric field, calculated from the measurement of the plasma current decay [2], reaches 30 V/m in the $E_{th} > 0.4$ MJ target plasmas and is larger than in the LFS MGI cases.

Nevertheless the increase of the effective electron density, $n_{eff} = n_e(t_0) + [1 + (Z-1) / 2] \int \Delta n_e(t)\, dt / \Delta t_{Feff}$, is larger than the increase of the corresponding n_c and the ratio n_{eff} / n_c is, in the range of N_{inj} explored, up to a factor of 2 larger than in the LFS MGI cases (t_0 is the trigger time, Z is the atomic number of the injected gas and the time-integral of the density increase is computed in Δt_{Feff}, that is between the thermal quench and the time at which $I_p = 0.2\, I_p(t_0)$).

Radiation asymmetry.

A large fraction of E_{th} is radiated during the cooling phase and the thermal quench, mostly in the sector of the valve. The AXUV diagnostic, which measures the spatial distribution of the radiated power, shows a very fast redistribution and penetration of the impurities into the plasma core during the thermal quench; the radiation emission during the current quench is toroidally symmetric.

Summary.

The F_{eff} of MGI from the HFS ranges between 35 and 55 % for moderate amounts (up to 20 % of what is needed to reach n_c) of injected neon and helium, which is a factor of two larger than F_{eff} reached with the fast valve close to the plasma located on the LFS. The improved performance of the HFS with respect to the LFS MGI motivates the installation of two valves behind the heat shield, in the attempt of reaching n_c.

References.

[1] T. Hender et al., Nuclear Fusion **47** (2007) S128

[2] G. Pautasso et al., Plasma Physics and Control Fusion **51** (2009) 124056

[3] H.W. Müller et al., Phys. Rev. Lett. **83** (1999) 2199–2202